phys. stat. sol. (c) **1**, No. 4, 1062–1066 (2004) / **DOI** 10.1002/pssc.200304217

# Nanostructured CdS:O film: preparation, properties, and application

**X. Wu**[*], **Y. Yan, R. G. Dhere, Y. Zhang, J. Zhou, C. Perkins,** and **B. To**

National Renewable Energy Laboratory, 1617 Cole Blvd., Golden, CO 80401, USA

Received 22 September 2003, revised 25 September 2003, accepted 28 November 2003
Published online 13 February 2004

**PACS** 68.55.–a, 73.63.–b, 78.66.Hf, 81.07.–b, 84.60.Jt

In this paper, we report on a novel material: nanostructured CdS:O film prepared at room temperature by rf sputtering, and its application in CdTe solar cells. The CdS:O film has a higher optical bandgap (2.5–3.1 eV) than the poly-CdS film and a nanostructure; the bandgap increases with an increase of oxygen content (from ~4 at.% to ~23 at.%) and a decrease of grain size (from about a few hundred Å to a few tenths Å). Our results have also demonstrated that the higher oxygen content presented in the nanostructured CdS:O films can significantly suppress the Te diffusion from the CdTe into the CdS film and the formation of a $CdS_{1-y}Te_y$ alloy with a lower bandgap that results in poor quantum efficiency in the short-wavelength region. The preliminary device results have demonstrated that the $J_{sc}$ of the CdTe device can be greatly improved by exploiting the thin nanostructured CdS:O film, while maintaining higher $V_{oc}$ and FF. We have fabricated a CdTe cell demonstrating an NREL-confirmed total-area efficiency of 15.5%.



**1 Introduction** Cadmium telluride (CdTe) has been recognized as a promising photovoltaic material for thin-film solar cells because of its near-optimum bandgap of ~1.5 eV and its high absorption coefficient. Small-area CdTe cells with efficiencies of more than 16% and commercial-scale modules with efficiencies of 11% have been demonstrated [1, 2]. However, the performance of CdTe cells has been limited by the conventional polycrystalline CdS/CdTe device structure. In the CdTe device, the poly-CdS film has been used most commonly as a window material. But it has three main issues that limit device performance. First, the $CdS_{1-y}Te_y$ alloy with lower bandgap can be formed between the CdTe and poly-CdS films, which affect device performance [3]. Second, poly-CdS film has a bandgap of ~2.42 eV, which causes considerable absorption in the short-wavelength region. Higher short-circuit current density ($J_{sc}$) can be achieved by reducing the CdS thickness to improve the blue spectral response. However, reducing the CdS thickness can adversely impact device open-circuit voltage ($V_{oc}$) and fill factor (FF). We have previously reported that by integrating a high-resistivity zinc stannate (ZTO) buffer layer between the poly-CdS and poly-CdTe films, we can minimize these detrimental effects [4]. Third, there is a nearly 10% lattice mismatch between the poly-CdTe film and the poly-CdS film, which causes the high defect density at the junction region. To reduce the lattice mismatch between the CdS and CdTe films, high-temperature device fabrication processes must be used to enhance the interdiffusion of the CdS and CdTe films and form intermixed layers ($CdS_{1-y}Te_y$ and $CdTe_{1-x}S_x$). But during the high-temperature processes, new defects and impurities are introduced that limit the improvement of device $V_{oc}$ and FF. Therefore, a new window material that has higher optical bangap, a better lattice match with the CdTe absorber, and minimum Te diffusion is an important project for further improving CdTe cell performance.

Several groups have developed new window materials with higher optical bandgaps than poly-CdS film, such as: ZnSe (2.69 eV), ZnS (3.70 eV), and $Zn_xCd_{1-x}S$ (2.42–3.70 eV) prepared by metal-organic chemical vapor deposition, spray pyrolysis, chemical-bath deposition, sputtering, and screen-printing

[*] Corresponding author: e:mail: xuanzhi_wu@nrel,gov, Phone: 303 384 6552, Fax: 303 384 6430

[5–7]. When using these window materials to replace the poly-CdS film, most device results show that $V_{oc}$ and FF are reduced, while $J_{sc}$ is improved. An explanation for this could be that these new poly window materials not only have higher bandgaps, but also have larger lattice mismatches to CdTe film than the poly-CdS film.

In this paper, we report on a novel window material: nanostructured CdS film (CdS:O) prepared at room temperature by rf sputtering. The CdS:O film has a higher optical bandgap and a smaller grain size than the poly-CdS film. The preliminary device results demonstrated that $J_{sc}$ of the CdTe device can be greatly improved, while maintaining higher $V_{oc}$ and FF.

**2 Preparation** The CdS:O films were prepared by rf magnetron sputtering at room temperature. The sputtering was carried out in a modified CVC SC-3000 system, evacuated to a base pressure of ~2–3x$10^{-6}$ torr and then backfilled with an oxygen/argon gas mixture at different ratios. Here, we refer to the $O_2$/Ar ratio as the ratio of its flow rates. A Corning 7059 glass substrate or glass/CTO ($Cd_2SnO_4$)/ZTO ($ZnSnO_x$) stack was placed on a sample holder parallel to the target surface. The distance between the substrate and the target was varied from 6 to 9 cm. In this study, we used a commercial hot-pressed CdS target with 99.99% purity. Depositions were performed at an $O_2$/Ar partial pressure of 10–20 x $10^{-3}$ torr with rf power between 50–70 watts, providing a deposition rate of 5–10 Å/s.

Five sputtered CdS samples (marked as samples #1–#5) were deposited at $O_2$/Ar ratios of 0%, 1%, 2%, 3% and 5%, respectively, on Corning 7059 glass substrates and used for material property characterizations. The electrical, optical, compositional, structural, and morphological properties of the CdS:O film were characterized using a Keithley 6517A electrometer, Cary 5 spectrophotometer, X-ray photoemission spectroscopy (XPS), transmission electron microscopy (TEM), energy-dispersive spectroscopy (EDS), and atomic force microscopy (AFM).

**3 Material properties**

**3.1 Electrical property** Table 1 lists light conductivities ($\sigma_L$), dark conductivities ($\sigma_D$), and photoconductivity ratios ($\sigma_L / \sigma_D$) of sputtered CdS films deposited at different $O_2$/Ar gas ratios. We can see from Table 1 that the maximum photoconductivity ratio of about 1000 is observed in samples #3 and #4, deposited at 2% and 3% $O_2$/Ar gas ratios, respectively. The CdS films (samples #3 and #4) with high photoconductivity ratios are suitable as a window layer in polycrystalline CdTe devices.

**Table 1** Electrical properties of sputtered CdS films deposited in different $O_2$/Ar gas mixtures.

| Sample # | $O_2$/Ar (%) | $\sigma_D$ (1/Ω cm) | $\sigma_L$ (1/Ω cm) | $\sigma_L / \sigma_D$ |
|---|---|---|---|---|
| 1 | 0 | $8.2\text{x}10^{-7}$ | $2.8\text{x}10^{-5}$ | 34 |
| 2 | 1 | $2.2\text{x}10^{-8}$ | $8.3\text{x}10^{-6}$ | 377 |
| 3 | 2 | $2.7\text{x}10^{-9}$ | $2.6\text{x}10^{-6}$ | 963 |
| 4 | 3 | $6.3\text{x}10^{-10}$ | $6.3\text{x}10^{-7}$ | 1000 |
| 5 | 5 | $4.3\text{x}10^{-9}$ | $1.2\text{x}10^{-7}$ | 30 |

**3.2 Optical property** The optical measurement results demonstrate that the optical bandgaps of sputtered film increase with the increase of $O_2$/Ar ratio (see Table 2). The nanostructured CdS films (such as samples #3, #4, and #5) have higher bandgaps than poly-CdS (such as sample #1), which can greatly help to improve device $J_{sc}$ and efficiency.

**Table 2** Optical bandgaps of sputtered CdS films deposited at different $O_2$/Ar gas mixtures.

| Sample # | $O_2$/Ar (%) | Optical bandgap (eV) |
|---|---|---|
| 1 | 0 | 2.42 |
| 2 | 1 | 2.52 |
| 3 | 2 | 2.65 |
| 4 | 3 | 2.80 |
| 5 | 5 | 3.17 |

**3.3 Compositional analysis (XPS data)** Table 3 lists oxygen atomic concentrations of sputtered films deposited at different $O_2$/Ar ratios. We observe that the oxygen atomic concentration in CdS films increases with increasing $O_2$/Ar ratio. Higher oxygen atomic concentration in CdS film can reduce Te diffusion from the CdTe to CdS film, thereby improving device $J_{sc}$ and efficiency [8].

**Table 3** The oxygen atomic concentration of sputtered CdS films deposited at different $O_2$/Ar ratios.

| Sample | $O_2$/Ar (%) | O (at.%) |
|---|---|---|
| 1 | 0 | 4.35 |
| 2 | 1 | 8.66 |
| 3 | 2 | 11.08 |
| 4 | 3 | 13.88 |
| 5 | 5 | 22.73 |

**3.4 Structural property** The microstructures of CdS thin films sputtered in oxygen-free (1#) and 2% oxygen environments (3#) were investigated by TEM. TEM samples were prepared by scratching small amounts of CdS films onto a Cu grid. The TEM images were taken on a Philips CM30 microscope, operated at 300 kV.

Figure 1(a) shows a bright-field image of a CdS film sputtered in an oxygen-free environment. The average grain sizes are found to be around 25 nm, which are consistent with the results from AFM [9]. Figure 1(b) shows a selected-area electron diffraction pattern taken from the same sample. It clearly reveals that the CdS film is polycrystalline.

Figure 2(a) shows a high-resolution TEM image of a CdS thin film sputtered in an 2% oxygen environment. The film is still polycrystalline, but average grain sizes are found to be around 3–5 nm, much smaller than the CdS film sputtered in oxygen-free environment. Figure 2(b) is a selected-area electron diffraction pattern, which was taken using the same select aperture as for Figure 1(b). It shows only diffraction rings, but not diffraction spots, indicating that the grain sizes are very small. Our TEM results suggest that one of the effects of oxygen in the growth environment is to reduce significantly the grain sizes of the sputtered CdS thin films, which results in the increase of their optical bandgap.

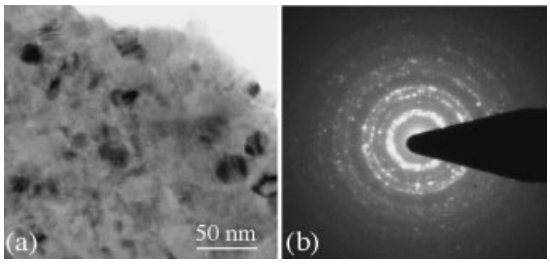


**Fig. 1** TEM and electron diffraction pattern of CdS film deposited in pure Ar (sample 1#).

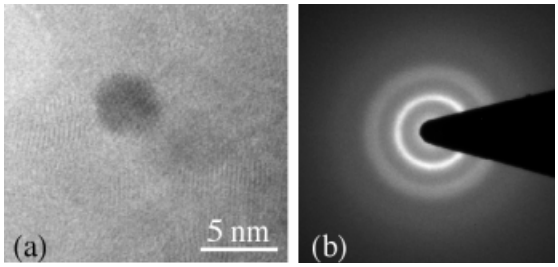


**Fig. 2** TEM and electron diffraction pattern of CdS film deposited in 2% $O_2$/Ar (sample 3#).

**4 Application in CdTe thin-film solar cells** A limited number of CdTe cells, with a modified CTO/ZTO/CdS:O/CdTe device structure, were prepared for demonstrating the application of nanostructured CdS:O films. CTO transparent conductive oxide (TCO) films and ZTO buffer layers were deposited in pure oxygen at room temperature, as previously described [1]. The CdS films were deposited in a 2% $O_2$/Ar gas mixture. The CdTe films were prepared by the close-spaced sublimation (CSS) technique and were deposited at 570°–630°C for 3 min. After CSS deposition of the CdTe, the substrates were treated in $CdCl_2$ vapor at 400°–430°C for 15 min. HgTe:CuTe-doped graphite paste, followed by a layer of Ag paste, was then applied to the devices as the back-contact layer.

We fabricated a number of CTO/ZTO/CdS:O/CdTe cells with NREL-confirmed efficiencies of more than 15% (see Table 4). It can be seen that when using a CdS:O film as the window layer, $J_{sc}$ of the CdTe device can be greatly improved, while maintaining higher $V_{oc}$ and FF.

**Table 4** High-efficiency CTO/ZTO/CdS:O/CdTe cells.

| Cell# | $V_{oc}$ (mV) | $J_{sc}$ (mA/cm$^2$) | FF (%) | $\eta$ (%) | Area (cm$^2$) |
|---|---|---|---|---|---|
| 1 | 821.1 | 25.71 | 72.55 | 15.3 | 1.166 |
| 2 | 832.4 | 25.85 | 71.77 | 15.4 | 1.056 |
| 3 | 837.1 | 24.36 | 75.30 | 15.4 | 1.137 |
| 4 | 832.4 | 24.67 | 75.27 | 15.5 | 0.965 |

It can be seen from Table 4 that high $J_{sc}$ values up to near 26 mA/cm$^2$ can be achieved by using the nanostructured CdS:O film. One of the effects of the CdS:O film is to significantly suppress the Te diffusion from the CdTe into the CdS film and minimize consumption of the CdS film that can allow use of thin CdS film in the CdTe cells.

Figures 3(a) and 3(b) show cross-sectional TEM images of a poly-CdS/CdTe cell (a) and a nanostructured CdS:O/CdTe cell (b). In the poly-CdTe cell, the CdS film with a polycrystalline structure was deposited in pure Ar by rf sputtering. In Fig. 3(a), the CdS layer is not visible in some regions, which indicates total consumption of the CdS film. In some areas, the CdS is seen, but with significantly decreased thickness, suggesting that the CdS consumption is spatially variable in the plane of the film. The EDS measurements (see Fig. 4[a]) also indicate Te diffusion into the CdS layer (point P1 in Fig. 4[a]). Optical bowing in the $CdS_{1-y}Te_y$ alloy system is such that small changes in the Te content of CdS can result in a large decrease in bandgap [10, 11]. The formation of $CdS_{1-y}Te_y$ alloy having a lower bandgap results in poor quantum efficiency in the short-wavelength region. In contrast, it can be seen that the nanostructured CdS:O layer is still very visible (see Fig. 3[b]). The nanostructured CdS:O film has much higher oxygen atomic concentration than poly-CdS film (see Table 3). Therefore, this strongly indicates that oxygen present in nanostructured CdS:O films significantly suppresses the Te interdiffusion from the CdTe to the CdS film and the formation of a $CdS_{1-y}Te_y$ alloy. The EDS results (see Fig. 4[b]) also confirm that Te cannot be found in the CdS:O layer (point P1 in Fig. 4[b]), which results in a high quantum efficiency in the short-wavelength region and a high $J_{sc}$.

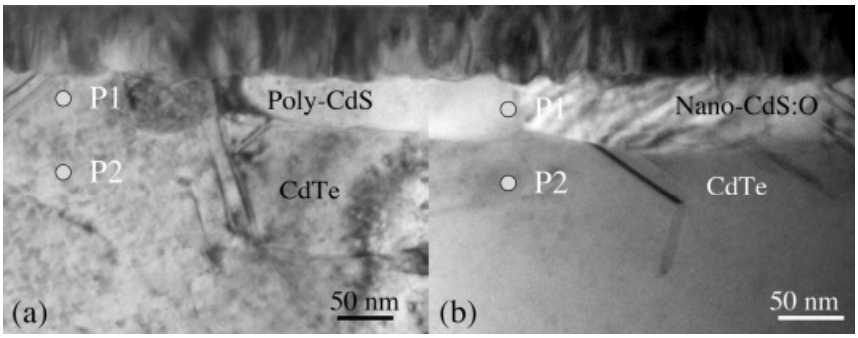


**Fig. 3** Cross-sectional TEM images of a poly-CdS/CdTe cell (a) and an a-CdS:O/CdTe cell (b).

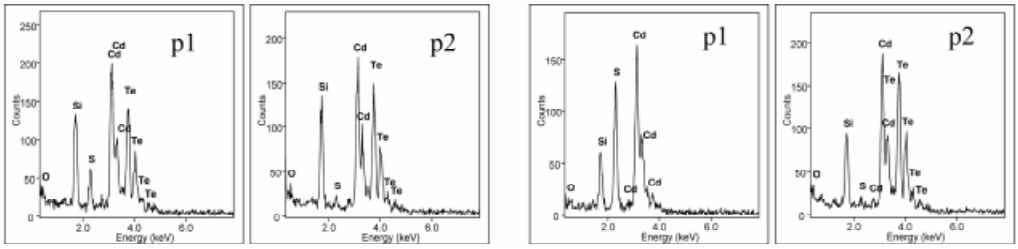


**Fig. 4** EDS (a) (left) and (b) (right) taken from points P1 and P2 marked on Fig. 3(a) and Fig. 3(b).

**5 Conclusions** We have developed a process for preparing the nanostructured CdS:O window material at room temperature by rf sputtering. The nanostuctured CdS : O films have a higher optical bandgap (2.5–3.1 eV) and a smaller grain size than the poly-CdS film, which results from its higher oxygen atomic concentration. The higher O content presented in the CdS : O films can significantly suppress the Te diffusion from the CdTe into the CdS film and the formation of a $CdS_{1-y}Te_y$ alloy, and minimize the consumption of the CdS film. When integrating the CdS : O film into a CdTe cell, the $J_{sc}$ can be greatly improved, while maintaining higher $V_{oc}$ and FF. A CdTe cell demonstrating an NREL-confirmed $J_{sc}$ of 25.85 mA/cm$^2$ and a total-area efficiency of 15.5% has been achieved.

**Acknowledgements** The authors would like to thank J. Keane, C. DeHart, G. Teeter, H.R. Moutinho, Q. Wang, T.A. Gessert, M.M. Al-Jassim, K. Zweibel, P. Sheldon, and J. Benner for their contributions and great support. This work is supported by the U.S. Department of Energy under Contract No. DE-AC36-99GO10337 to NREL.

## References

[1] X. Wu et al., Proc of 17th European PVSEC, p. 995 (2001).
[2] D. Cunningham et al., Proc. of 28th IEEE PVSC, p. 13–18 (2000).
[3] B. E. McCandless et al., Proc of 22nd IEEE PVSC, p. 967 (1991).
[4] X. Wu et al., J. Appl. Phys. **89 (8)**, 4564 (2001).
[5] T. L. Chu et al., J. Appl. Phys. **71**, 3865 (1992).
[6] C. S. Ferekides et al., Proc. of 13th NREL PV Program Review Meeting, p. 39 (1995).
[7] I. O. Oladeji et al., Solar Energy Materials & Solar Cells, **61**, 203 (2000).
[8] Y. Yan et al., Proc. of NREL/SNL PV Program Review Meeting (2001).
[9] X. Wu et al., Proc of 29th IEEE PVSC, p. 531 (2002).
[10] K. Ohata et al., Jpn. J. Appl. Phys. **12 (10),** 1641 (1973).
[11] S. Wei et al., J. Appl. Phys. **87 (3)**, 1304 (2000).